J Supercond Nov Magn (2016) 29:1813–1819
DOI 10.1007/s10948-016-3462-x

ORIGINAL PAPER

A Novel Theoretical Investigation of Electronic Structure and Half-Metallic Ferromagnetism in 3d (V)-Doped InP for Spintronic Applications

Yacine Cherfi[1] · Allel Mokaddem[2] · Djillali Bensaid[3] · Bendouma Doumi[4] · Adlane Sayede[5] · Fethallah Dahmane[6] · Abdelkader Tadjer[7]

Received: 6 February 2016 / Accepted: 12 February 2016 / Published online: 27 February 2016

Abstract We have investigated the electronic structure and half-metallic ferromagnetic properties of vanadium (V)-doped InP indium phosphide in the zinc blende structure as ternary $In_{1-x}V_xP$ compounds at concentrations $x = 0.25$, 0.5, and 0.75 of V, using first-principles calculations of density functional theory with generalized gradient approximation functional of Wu and Cohen (GGA-WC). It is found that $In_{0.75}V_{0.25}P$, $In_{0.5}V_{0.5}P$, and $In_{0.25}V_{0.75}P$ compounds depicted a half-metallic (HM) ferromagnetic character with spin polarization of 100 % at Fermi level. The HM ferromagnetic behavior is confirmed by the integral Bohr magneton of total magnetic moment of 2 μ_B per V atom of $In_{1-x}V_xP$, which mainly arises from the *3d* (V) states along with less important contributions of induced local magnetic moments at In and P sites. Therefore, the $In_{1-x}V_xP$ material seems to be potential candidate for possible semiconductor spintronics applications.

Keywords First-principles calculations · V-doped InP · Electronic structure · Half-metallic ferromagnets · Spintronics

✉ Bendouma Doumi
bdoummi@yahoo.fr

1 Faculty of Physics, Theoretical Physics Laboratory, U.S.T.H.B., Algiers, Algeria

2 Faculty of Physics, Department of Materials and Components, U.S.T.H.B., Algiers, Algeria

3 Laboratory Physico-Chemistry of Advanced Materials, Djillali Liabes University of Sidi Bel-Abbes, 22000 Sidi Bel-Abbes, Algeria

4 Faculty of Sciences, Department of Physics, Dr. Tahar Moulay University of Saïda, 20000 Saïda, Algeria

5 Unité de Catalyse et Chimie du Solide (UCCS), UMR CNRS 8181, Faculté des Sciences, Université d'Artois, Rue Jean Souvraz, SP 18, 62307 Lens, France

6 Institut des Sciences et Technologies, Département Sciences de la Matière, Centre Universitaire Tissemsilt, 38000 Tissemsilt, Algérie

7 Modelling and Simulation in Materials Science Laboratory, Physics Department, Djillali Liabes University of Sidi Bel-Abbes, 22000 Sidi Bel-Abbes, Algeria

1 Introduction

In electronics, electrical charges are used to store information and perform logic operations; however in addition to their charges, electrons have magnetic moments (spins), but this property is not used in conventional solid-state electronic devices [1, 2] Since the existence of spintronics (spin transport electronics or spin-based electronics) is a new generation of microelectronics [3–5], which exploits the spin of charge carriers in the emerging field of promising materials for spin-based multifunctional devices The development of diluted magnetic semiconductors (DMSs) based on III–V and II–VI semiconductors doped with transition metal atoms has attracted increasing interest in recent years due to their possible usage in spintronics applications [6–18]. The DMS materials are characterized by the Curie temperatures higher than room temperature and half-metallic ferromagnetic (HMF) behavior [19]. The DMS electronic structures have spin-polarized carriers, resulting in variation of density of states of majority spin and minority spin at Fermi level (E_F) and thus they behave a metallic nature in one spin

direction and a band gap at the Fermi level in the opposite spin channel The spin polarization of a system at E_F can be defined as [20]

$$P = \frac{N^{\uparrow}(E_F) - N^{\downarrow}(E_F)}{N^{\uparrow}(E_F) + N^{\downarrow}(E_F)} \quad (1)$$

where the $N^{\uparrow}(E_F)$ and $N^{\downarrow}(E_F)$ are the spin-polarized density of states at (E_F) of majority spin and minority spin, respectively. de Groot et al. [21] have discovered the concept of half-metallic ferromagnetism as a material revealing a gap in one spin direction and metallic character in the other spin channel, which leads to a spin polarization of $P = 1$ when $N^{\uparrow}(E_F)$ or $N^{\downarrow}(E_F)$ equals zero; this yields a carrier spin polarization of 100 % at E_F [22].

The indium phosphide (InP) belong to the III–V group that crystallize in the zinc blende phase; it is an important semiconductor due to its significant physical properties and good characteristics for various applications such as attractive for long-wavelength optoelectronics and for high-speed and high-power electronic devices [23]; it has used as a substrate for high-speed electrical and optoelectronic device like high frequency field effect transistors and resonant interband tunneling diodes [24, 25].

The InP is a perfect modern semiconductor for selective spin excitation by circular-polarized photons due to its direct band gap (1.34 eV) [26]. It has received significant attention as a possible candidate DMS material according to a theoretical study of T. Dietl et al. [27] which predicted the Curie temperature TC for p-type InP containing 5 % of Mn and 3.5×10^{20} holes per cm^3 and to the experimental report of J. Hollingsworth et al. [28] that found the highest Tc (∼130 K) in Mn-doped InP. The ferromagnetism Mn-Mn coupling has theoretically reported for Mn-doped InP nanowires [29], and the Mn^{+3} center in InP has various properties of a well-localized center and some of a weakly localized one [30]. Besides, the Mn is a relatively deep acceptor in III–Mn–V, and its level in InP is 0.22 eV above the valence band maximum [31]. Recently, the half-metallic ferromagnetism is theoretically predicted in $In_{1-x}Cr_xP$ and $In_{1-x}Mn_xP$ [32] and the Mn-Doped InP nanowire [33].

In the present work, we have studied the electronic and ferromagnetic properties of zinc blende $In_{1-x}V_xP$ at concentrations $x = 0.25$, 0.5, and 0.75 of vanadium (V), based on simple ordered In_3VP_4, $In_2V_2P_4$, and InV_3P_4 supercells 8 atoms. We have used first-principles calculations of density functional theory [34, 35] within the framework of full-potential linearized augmented plane wave method to investigate the electronic structure, half-metallic ferromagnetic behavior, and the mechanism responsible for creation of ferromagnetism in $In_{1-x}V_xP$.

2 Method of Calculations

The calculations are carried out using the framework of the density functional theory (DFT) [34, 35] within the full-potential linearized augmented plane wave (FP-LAPW) method as implemented in WIEN2K package [36]. The exchange correlation potential was treated by using the generalized gradient approximation functional of Wu and Cohen (GGA-WC) [37]. We have determined the structural parameters, electronic and magnetic properties of InP semiconducteur in zinc blende structure doped with transition metal vanadium (V) impurity as ternary $In_{1-x}V_xP$ compounds at concentrations $x = 0.25$, 0.5, and 0.75.

We have chosen the averages of non-overlapping muffin-tin radii (R_{MT}) of In, P and V in such a way that the muffin-tin spheres do not overlap. The wave functions are expanded in the interstitial region to plane waves with a cutoff of $K_{max} = 8.0/R_{MT}$ (where K_{max} is the magnitude of the largest K vector in the plane wave and R_{MT} is the average radius of the muffintin spheres), and the maximum value for partial waves inside the atomic sphere was $l_{max} = 10$, while the charge density was Fourier expanded up to $G_{max} = 12$, where G_{max} is the largest vector in the Fourier expansion. For the sampling of the Brillouin zone, we used the Monkhorst–Pack mesh [38, 39] of $(4 \times 4 \times 4)$ k-points for InP, $In_{0.75}V_{0.25}P$ and $In_{0.25}V_{0.75}P$ and $(4 \times 4 \times 3)$ k-points for $In_{0.5}V_{0.5}P$, where the self-consistent convergence of the total energy was set at 0.1 mRy.

3 Results and Discussions

3.1 Optimization of Crystal Structures

The InP has zinc blende (B3) structure with space group of $F\bar{4}3m$ No. 216, where the In atom and P atom are located at (0, 0, 0) and (0.25, 0.25, 0.25) positions, respectively. The concentrations 0.25, 0.5, and 0.75 are obtained by substituted of one, two, and three In cation sites, respectively, by V impurities in In_4P_4 supercell of 8 atoms. We get the $In_{0.5}V_{0.5}P$ $(1 \times 1 \times 1)$ supercell of 8 atoms with $x = 0.5$ of tetragonal structure with space group $P\bar{4}m2$ No. 115, and the $In_{0.75}TM_{0.25}P$ $(1 \times 1 \times 1)$ and $In_{0.25}TM_{0.75}P$ $(1 \times 1 \times 1)$ standard unit cells of 8 atoms are obtained respectively for $x = 0.25$ and 0.75 with cubic structure and space group $P\bar{4}3m$ No. 215.

In order to calculate the structural parameters of $In_{1-x}V_xP$ compounds, we have fitted the variations of total energies as a function of equilibrium volumes with the empirical Murnaghan's equation of state [40]. Our results of equilibrium lattice constants (a) and bulk modules (B) for pure InP and $In_{1-x}V_xP$ at concentrations $x = 0.25$, 0.5 and

Table 1 Calculated lattice constant (a) and bulk modulus (B) for InP $In_{0.875}V_{0.125}P$ $In_{0.75}V_{0.25}P$, $In_{0.5}V_{0.5}P$ and $In_{0.25}V_{0.75}P$

Compound	a (Å)		B (GPa)	
InP	5.892	5.893[a] 5.890[b], 5.869[c]	66.28	66.55[a], 67.40[b], 72.00[d]
$In_{0.75}V_{0.25}P$	5.788		71.78	
$In_{0.5}V_{0.5}P$	5.674		80.55	
$In_{0.25}V_{0.75}P$	5.558		101.92	

[a]Theoretical values from Ref. [32]
[b]Theoretical values from Ref. [41]
[c]Experimental values from Ref. [42]
[d]Experimental values from Ref. [43]

0.75, various theoretical [32, 41] and experimental [42, 43] data are summarized in Table 1. The calculated lattice constant of InP is very close to the theoretical calculations [32, 41] by the same GGA-WC method [37] and stay in agreement with the experimental data due to better performance of GGA-WC method for optimization of structures [1, 2, 44–46], resulting from the fourth-order gradient expansion of exchange correlation functional [37, 45].

Owing to the difference between the ionic radii of V and In atoms, the lattice parameter of ternary $In_{1-x}V_xP$ compound decreases with an increasing concentration (x) of vanadium (V) impurity. As a consequence, the bulk modulus

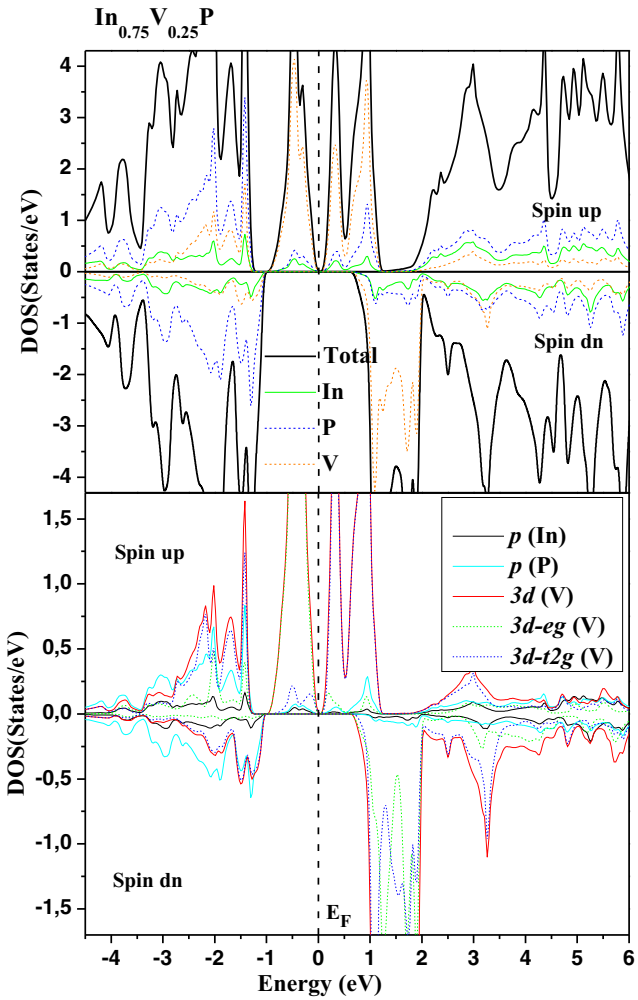

Fig. 1 Spin-polarized total and partial DOS of $In_{0.75}V_{0.25}P$. The Fermi level is set to zero (*vertical dotted line*)

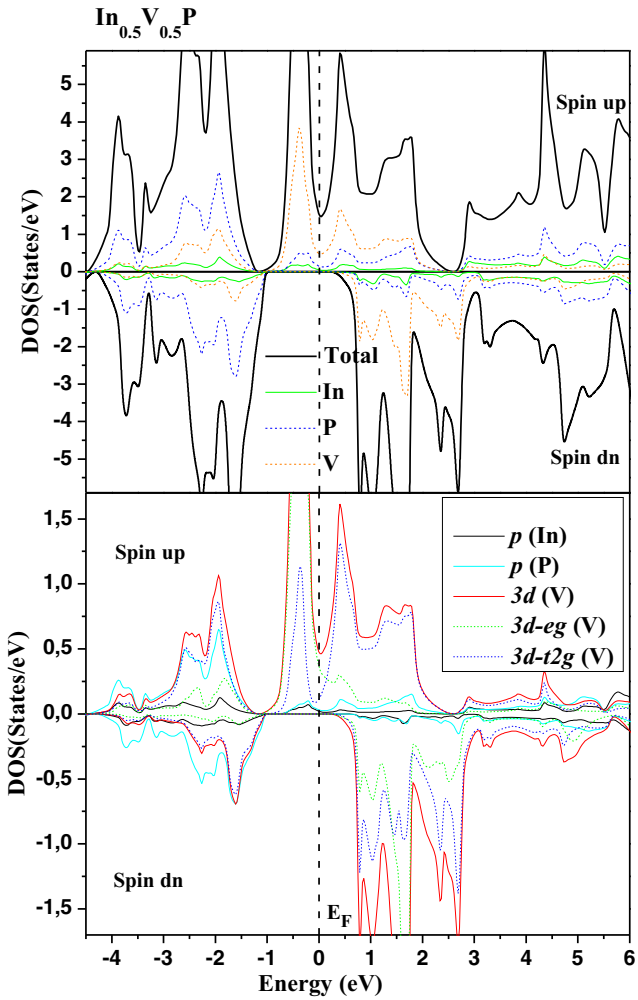

Fig. 2 Spin-polarized total and partial DOS of $In_{0.5}V_{0.5}P$. The Fermi level is set to zero (*vertical dotted line*)

increases and $In_{1-x}V_xP$ becomes harder when the concentration (x) of (V) increases. We have noted that there are no experimental and theoretical works of structural parameters for $In_{1-x}V_xP$ to compare with the results of our work. In the next, we have used the computed lattice constants of $In_{1-x}V_xP$ compounds to determine their electronic and magnetic properties.

3.2 Electronic Properties

To investigate the electronic properties and the origin of ferromagnetism in compounds under study, we have performed the spin-polarized electronic structures. Figures 1, 2, and 3 displayed the total (T) and partial (P) density of states (DOS) for $In_{0.75}V_{0.25}P$, $In_{0.5}V_{0.5}P$ and $In_{0.25}V_{0.75}P$, respectively, and the spin-polarized band structures are presented in Figs. 4, 5, and 6, respectively for $In_{0.75}V_{0.25}P$, $In_{0.5}V_{0.5}P$ and $In_{0.25}V_{0.75}P$. The all TDOS and band structures show clearly that majority spin states are metallic and minority

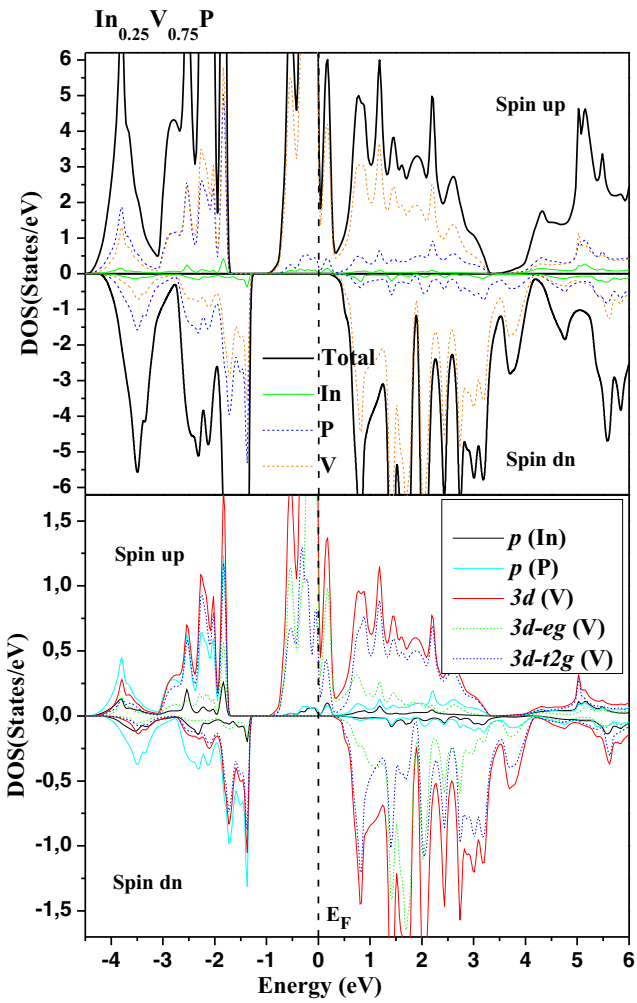

Fig. 3 Spin-polarized total and partial DOS of $In_{0.25}V_{0.75}P$. The Fermi level is set to zero (*vertical dotted line*)

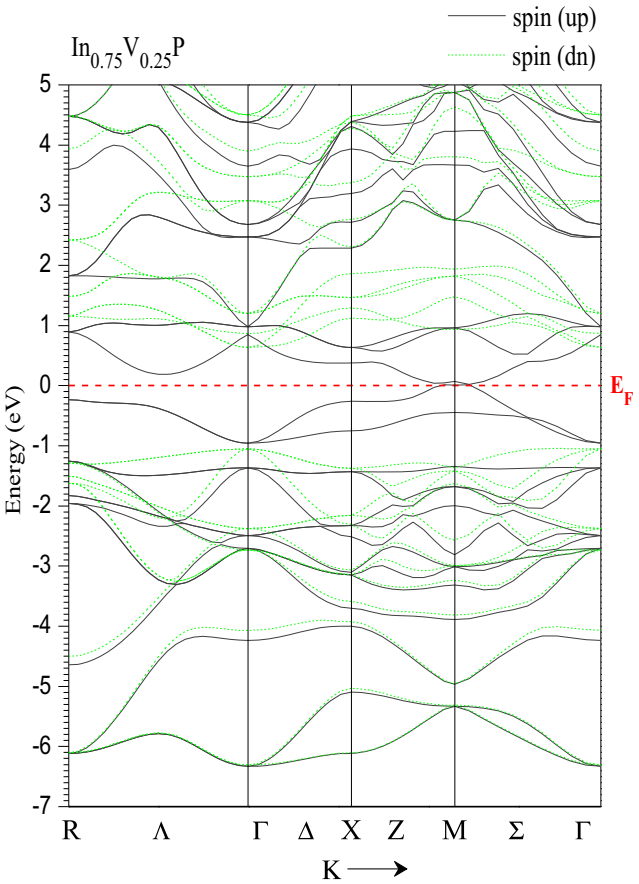

Fig. 4 Spin-polarized band structures of majority spin (*up*) and minority spin (*dn*) for $In_{0.75}V_{0.25}P$. The Fermi level is set to zero (*horizontal dotted line*)

spin states have gaps at Fermi level (E_F), which implies that $In_{1-x}V_xP$ compounds are half-metallic ferromagnets with spin polarization of 100 %. The metallic character of majority spin results from the strong hybridization between p (P) and $3d$ (V) that crosses E_F, while the DOS disappear at E_F for minority spin.

Based on the crystal field theory [47] and due to crystal field created by the (P) ions, we have depicted from TDOS that 3d (V) states are divided into twofold generate low-lying $e_g(d_{z^2}$, and $d_{x^2-y^2})$ and the threefold degenerate high-lying $t_{2g}(d_{xy}d_{xz}$, and $d_{yz})$ symmetry states. Therefore, we understand that the V atom is situated in tetrahedral surroundings of P neighboring. As well, we have noticed that hybridization of p (P) and 3d (V) states occurs at E_F for majority spin of $In_{1-x}V_xP$, mining that these states are metallic, but there are no states at E_F for minority spin of $In_{1-x}V_xP$. The DOS of the top of majority spin valence bands and the bottom of minority spin conduction bands are mainly formed by the p (P) and 3d (V) states for $In_{0.75}V_{0.25}P$, $In_{0.5}V_{0.5}P$ and $In_{0.25}V_{0.75}P$. In contrast, the contribution of p (In) states is minor in valence and

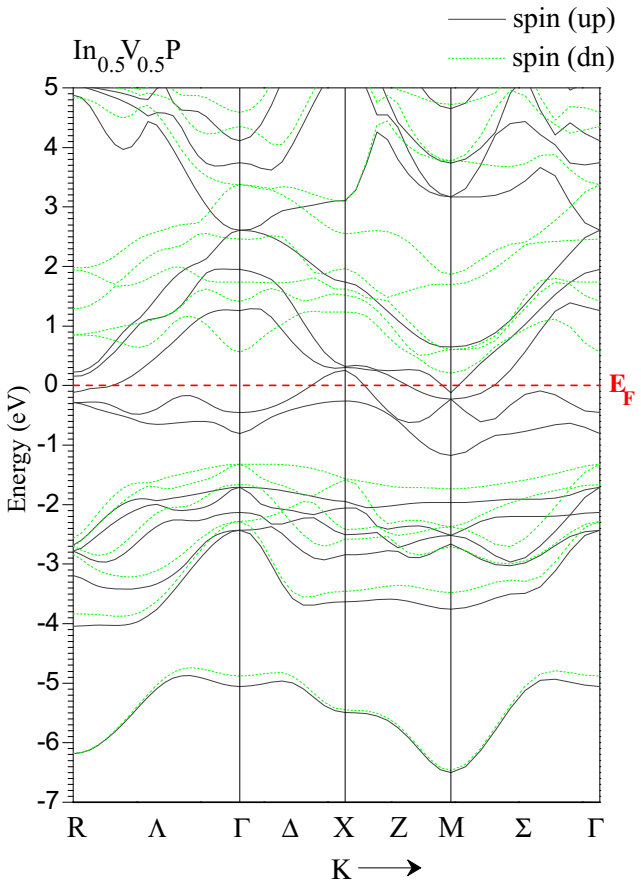

Fig. 5 Spin-polarized band structures of majority spin (*up*) and minority spin (*dn*) for $In_{0.5}V_{0.5}P$. The Fermi level is set to zero (*horizontal dotted line*)

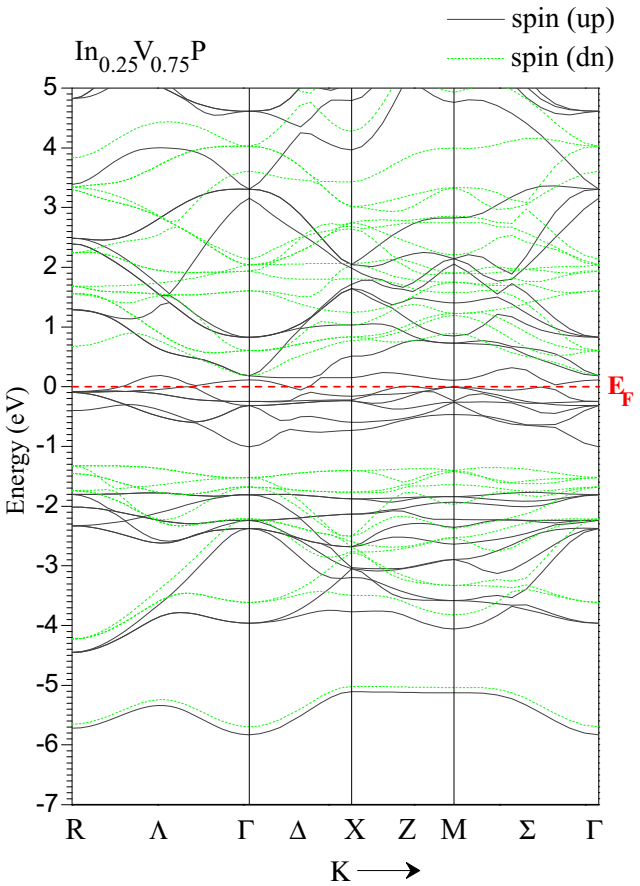

Fig. 6 Spin-polarized band structures of majority spin (*up*) and minority spin (*dn*) for $In_{0.25}V_{0.75}P$. The Fermi level is set to zero (*horizontal dotted line*)

conduction bands of both majority spin and minority spin channels.

Moreover, the stability of ferromagnetic state in DMS-based III–V and II–VI semiconductors doped with transition metal (TM) elements is explained by the double-exchange mechanism when the 3d (TM) anti-bonding states are partially filled [48–51]. In the V-doped InP (III–V) type, we suggested that 3d (V) partially occupied majority spin states lower the total energies of $In_{1-x}V_xP$ doping systems and stabilize a ferromagnetic state arrangement associated with the double-exchange mechanism [52]. We know that the stabilization of ferromagnetic ground state of $In_{1-x}V_xP$ compounds is due to the contribution of both $p-d$ exchange and double-exchange mechanisms.

Furthermore, the half-metallic ferromagnetic (HMF) gap (E_{HMF}) and half-metallic (HM) gap (flip-gap) (G_{HM}) for minority spin states are given in Table 2. Figures 4, 5, and 6 demonstrate that minority spin bands have direct HMF gaps at the Γsymmetry point; it is 1.688, 1.882 and 1.712 for $In_{0.75}V_{0.25}P$, $In_{0.5}V_{0.5}P$ and $In_{0.25}V_{0.75}P$, respectively. For majority spin bands, the valence band formed by the 3d (V) states broaden more strongly in gap when the concentration (x) of V increases, which overlapped with the conduction bands. This leads to metallic nature for majority spin bands The HM gap (flip-gap) determines the minimal energy band gap for a spin-flip excitation required for generating a hole or an electron in minority spin [1, 15]; it is an important parameter that determines the usage of DMS materials for spintronics [53]. This parameter is defined as the minimum between the lowest energy of majority (minority)-spin conduction bands with respect to the Fermi level and the absolute values of the highest energy of majority (minority)-

Table 2 Calculated half-metallic ferromagnetic band gap (E_{HMF}) and half-metallic gap (G_{HM}) of minority spin bands for $In_{0.75}V_{0.25}P$, $In_{0.5}V_{0.5}P$ and $In_{0.25}V_{0.75}P$

Compound	E_{HMF} (eV)	G_{HM} (eV)
$In_{0.75}V_{0.25}P$	1.688	0.636
$In_{0.5}V_{0.5}P$	1.882	0.561
$In_{0.25}V_{0.75}P$	1.712	0.187

Table 3 Calculated total and local magnetic moments per V atom (in Bohr magneton μ_B) within the muffin-tin spheres and in the interstitial sites for $In_{0.75}V_{0.25}P$, $In_{0.5}V_{0.5}P$ and $In_{0.25}V_{0.75}P$

Compound	Total (μ_B)	V (μ_B)	In (μ_B)	P (μ_B)	Interstitial (μ_B)
$In_{0.75}V_{0.25}P$	2	1.888	0.037	−0.178	0.255
$In_{0.5}V_{0.5}P$	2	1.840	0.022	−0.153	0.293
$In_{0.25}V_{0.75}P$	2	1.812	0.012	−0.012	0.316

spin valence bands [54, 55]. However, the flip-gaps are 0.636, 0.561, and 0.187 eV, respectively, for $In_{0.75}V_{0.25}P$, $In_{0.5}V_{0.5}P$ and $In_{0.25}V_{0.75}P$ located between Fermi level (0 eV) and the conduction bands minimum of minority spin, which describe the smallest gap for generating an electron in minority spin conduction bands. Besides, the large flip-gap shapes a true half-metallic, and thus, it is understandable from the foregoing that $In_{1-x}V_xP$ material at concentration $x = 0.25$ seems to be the best promising candidate than the other $In_{1-x}V_xP$ compounds at $x = 0.5$ and 0.75 for possible future semiconductor spintronics applications.

3.3 Magnetic Properties

The $In_{1-x}V_xP$ compounds are obtained by substituted of indium (In) cation sites with vanadium (V) $4s^2 3d^3 (e_g^2 t_{2g}^1)$ atoms, where each V atom contributes three electrons to bonding states of host valence bands. As result, the configuration of valence band of vanadium impurity in $In_{1-x}V_xP$ becomes V^{+3} $4s^0 3d^2 (e_g^2\, t_{2g}^0)$. According to the Hund's rule, the *3d* (V) minority spin states are empty, whereas the *3d* (V) majority spin are partially filled with two electrons; two in e_g (V) states and empty electrons in t_{2g} (V) states. The two unpaired electrons of e_g (V) states create a total magnetic moment of 2 μ_B per V atom (μ_B is the Bohr magneton) for each $In_{1-x}V_xP$ compound. The integral of Bohr magneton of 2 μ_B, means that $In_{0.75}V_{0.25}P$, $In_{0.5}V_{0.5}P$, and $In_{0.25}V_{0.75}P$ are true half-metallic ferromagnets.

The total (T) and local (L) magnetic moments (MMs) per V atom within the muffin-tin spheres of the relevant atoms and in the interstitial sites for $In_{1-x}V_xP$ compounds are listed in Table 3. The major contributions of TMMs are localized on LMMs of V atoms, and these LMMs are smaller than 2 μ_B of Hund's rule due to $p - d$ exchange interaction between *p* (P) and *3d* (V) orbitals. Also, the smaller LMMs are induced on the nonmagnetic In and P sites. On the other hand, the magnetic spins interaction is determined by the sign of magnetic moment of each atom. In our case, the negative signs of LMMs of (P) atoms describe the anti-ferromagnetic interaction between vanadium (V) and valence bands having *p* (P) character, but the ferromagnetic interaction between vanadium (V) and indium (In) magnetic spins is revealed by the positives LMMs of In atoms.

4 Conclusion

The first-principle calculations of DFT within the FP-LAPW method with GGA-WC approximation have been used to study the electronic and magnetic properties of $In_{1-x}V_xP$ at concentrations $x = 0.25$, 0.5, and 0.75 in zinc blende phase. We have reached that $In_{1-x}V_xP$ are half-metallic (HM) ferromagnets with 100 % spin polarization. The HM gaps are 0.636, 0.561, and 0.187 eV, respectively, for $In_{0.75}V_{0.25}P$, $In_{0.5}V_{0.5}P$, and $In_{0.25}V_{0.75}P$ with total magnetic moments of 2 μ_B per V atom, confirming the true half-metallic ferromagnetic behavior of these compounds. However, the ferromagnetic state in $In_{1-x}V_xP$ originated from both double-exchange and $p - d$ exchange mechanisms. The $In_{1-x}V_xP$ is predicted to be a promising DMS material for possible semiconductor spintronics applications.

References

1. Doumi, B., Mokaddem, A., Dahmane, F., Sayede, A., Tadjer, A.: RSC Adv. **112**, 92328 (2015)
2. Doumi, B., Mokaddem, A., Sayede, A., Dahmane, F., Mogulkoc, Y., Tadjer, A.: Superlattices Microstruct. **88**, 139 (2015)
3. Wolf, S.A., Awschalom, D.D., Buhrman, R.A., Daughton, J.M., von Molnár, S., Chtchelkanova, A.Y., Treger, T.M.: Science **294**, 1488 (2001)
4. Žutić, I., Fabian, J., DasSarma, S.: Rev. Mod. Phys. **76**, 323 (2004)
5. Doumi, B., Tadjer, A., Dahmane, F., Mesri, D., Aourag, H.: J. Supercond. Nov. Magn **26**, 515 (2013)
6. Rajamanickam, N., Rajashabala, S., Ramachandran, K.: Superlattices Microstruct. **65**, 240 (2014)
7. Rajendar, V., Dayakar, T., Shobhan, K., Srikanth, I., Venkateswara Raom K.: Superlattices Microstruct. **75**, 551 (2014)
8. Singh, J., Verma, N.K.: J. Supercond. Nov. Magn. **27**, 2371 (2014)
9. Kaur, P., Kumar, S., Singh, A., Chen, C.L., Dong, C.L., Chan, T.S., Lee, K.P., Srivastava, C., Rao, S.M., Wu, M.K.: Superlattices Microstruct. **83**, 785 (2015)
10. Boutaleb, M., Doumi, B., Sayede, A., Tadjer, A., Mokaddem, A.: J. Supercond. Nov. Magn. **28**, 143 (2015)
11. Wang, S.F., Chen, L.Y., Zhang, T., Song, Y.L.: J. Supercond. Nov. Magn. **28**, 2033 (2015)
12. Doumi, B., Mokaddem, A., Ishak-Boushaki, M., Bensaid, D.: Sci. Semicond. Process **32**, 166 (2015)
13. Shayesteh, S.F., Nosrati, R.: J. Supercond. Nov. Magn. **28**, 1821 (2015)
14. Saini, H.S., Kashyap, M.K., Kumar, M., Thakur, J., Singh, M., Reshak, A.H., Saini, G.S.S.: J. Alloy. Compd. **649**, 184 (2015)

15. Doumi, B., Mokaddem, A., Temimi, L., Beldjoudi, N., Elkeurti, M., Dahmane, F., Sayede, A., Tadjer, A., Ishak-Boushaki, M.: Eur. Phys. J. B **88**, 93 (2015)
16. Kervan, S., Kervan, N.: J. Magn. Magn. Mater **382**, 63 (2015)
17. Boutaleb, M., Doumi, B., Sayede, A., Tadjer, A.: J. Magn. Magn. Mater **397**, 132 (2016)
18. Mahmood, Q., Alay-e-Abbas, S.M., Yaseen, M., Mahmood, A., Rashid, M., Noor, N.A. J. Supercond. Nov. Magn. doi:10.1007/s10948-016-3434-1
19. Mokaddem, A., Doumi, B., Sayede, A., Bensaid, D., Tadjer, A., Boutaleb, M.: J. Supercond. Nov. Magn. **28**, 157 (2015)
20. Soulen, R.J., Byers, J.M., Osofsky, M.S., Nadgorny, B., Ambrose, T., Cheng, S.F., Broussard, P.R., Tanaka, C.T., Nowak, J., Moodera, J.S., Barry, A., Coey, J.M.D.: Science **282**, 85 (1998)
21. de Groot, R.A., Mueller, F.M., van Engen, P.G., Buschow, K.H.J.: Phys. Rev. Lett. **50**, 2024 (1983)
22. De Boeck, J., Van Roy, W., Das, J., Motsnyi, V., Liu, Z., Lagae, L., Boeve, H., Dessein, K., Borghs, G.: Semicond. Sci. Technol. **17**, 342 (2002)
23. Gorodynskyy, V., Zdansky, K., Pekarek, L., Malina, V., Vackova, S.: Nucl. Instr. Meth. A **555**, 288 (2005)
24. Werking, J.D., Bolognesi, C.R., Chang, L.-D., Nguyen, C., Hu, E.L., Kroemer, H.: IEEE Electron Dev. Lett. **13**, 164 (1992)
25. Soderstrom, J.R., Chow, D.H., McGill, T.C.: Appl. Phys. Lett. **55**, 1094 (1989)
26. Caspers, C., Yoon, D., Soundararajan, M., Ansermet, J.-P.: New. J. Phys. **17**, 022004 (2015)
27. Dietl, T., Ohno, H., Matsukara, F., Cibert, J., Ferrand, D.: Science **287**, 1019 (2000)
28. Hollingsworth, J., Bandaru, P.R.: Mater. Sci. Eng. B **151**, 152 (2008)
29. Schmidt, T.M., Venezuela, P., Arantes, J.T., Fazzio, A.: Phys. Rev. B **73**, 235330 (2006)
30. Korona, K.P., Wysmolek, A., Kamińska, M., Twardowski, A., Piersa, M., Palczewska, M., Strzelecka, G., Hruban, A., Kuhl, J., Adomavicius, R., Krotkus, A.: Physica B **382**, 220 (2006)
31. Tarhan, E., Miotkowski, I., Rodriguez, S., Ramdas, A.K.: Phys. Rev. B **67**, 195202 (2003)
32. Boutaleb, M., Tadjer, A., Doumi, B., Djedid, A., Yakoubi, A., Dahmane, F., Abbar, B.: J. Supercond. Nov. Magn. **27**, 1603 (2014)
33. Srivastava, P., Kumar, A., Jaiswal, N.K.: Superlattices Microstruct. doi:10.1016/j.spmi.2016.01.039
34. Hohenberg, P., Kohn, W.: Phys. Rev. B **136**, 864 (1964)
35. Kohn, W., Sham, L.J.: Phys. Rev. A **140**, 1133 (1965)
36. Blaha, P., Schwarz, K., Madsen, G.K.H., Kvasnicka, D., Luitz, J.: WIEN2k, An augmented plane wave plus local orbitals program for calculating crystal properties. Vienna University of Technology, Vienna (2001)
37. Wu, Z., Cohen, R.E.: Phys. Rev. B **73**, 235116 (2006)
38. Monkhorst, H.J., Pack, J.D.: Phys. Rev. B **13**, 5188 (1976)
39. Pack, J.D., Monkhorst, H.J.: Phys. Rev. B **16**, 1748 (1977)
40. Muranghan, F.D.: Proc. Natl. Acad. Sci. U.S.A. **30**, 244 (1944)
41. Tran, F., Laskowski, R., Blaha, P., Schwarz, K.: Phys. Rev. B **75**, 115131 (2007)
42. Heyd, J., Peralta, J.E., Scuseria, G.E., Martin, R.L.: J. Chem. Phys. **123**, 174101 (2005)
43. Wang, S.Q., Ye, H.Q.: Phys. Rev. B **66**, 235111 (2002)
44. Sharma, S., Verma, A.S., Bhandari, R., Kumari, S., Jindal, V.K.: Mater. Sci. Semicond. Process **27**, 79 (2014)
45. Sajjad, M., Manzoor, S., Zhang, H.X., Noor, N.A., Alay-e-Abbas, S.M., Shaukat, A., Khenata, R.: J. Magn. Magn. Mater. **379**, 63 (2015)
46. Doumi, B., Mokaddem, A., Sayede, A., Boutaleb, M., Tadjer, A., Dahmane, F.: J. Supercond. Novel Magn. **28**, 3163 (2015)
47. Zunger, A.: Solid State Phys. **39**, 275 (1986)
48. Sato, K., Katayama-Yoshida, H.: Jpn. J. Appl. Phys. **40**, L485 (2001)
49. Sato, K., Katayama-Yoshida, H.: Semicond. Sci. Technol. **17**, 367 (2002)
50. Sato, K., Katayama-Yoshida, H., Dederichs, P.H.: J. Supercond **16**(1), 31 (2003)
51. Sato, K., Dederichs, P.H., Araki, K., Katayama-Yoshida, H.: Phys. Status Solidi C **7**, 2855 (2003)
52. Akai, H.: Phys. Rev. Lett **81**, 3002 (1998)
53. Doumi, B., Tadjer, A., Dahmane, F., Djedid, A., Yakoubi, A., Barkat, Y., Ould Kada, M., Sayede, A., Hamada, L.: J. Supercond. Nov. Magn. **27**, 293 (2014)
54. Yao, K.L., Gao, G.Y., Liu, Z.L., Zhu, L.: Solid State Commun. **133**, 301 (2005)
55. Gao, G.Y., Yao, K.L., Şaşıoğlu, E., Sandratskii, L.M., Liu, Z.L., Jiang, J.L.: Phys. Rev. B **75**, 174442 (2007)